Available online at www.sciencedirect.com
SCIENCE DIRECT®
Journal of Nuclear Materials 343 (2005) 212–218
journal of nuclear materials
www.elsevier.com/locate/jnucmat

Micro-hardness measurement and micro-structure characterization of T91 weld metal irradiated in SINQ Target-3

X. Jia *, Y. Dai

Paul Scherrer Institut, CH-5232 Villigen, Switzerland

Abstract

This work is concerned with the micro-structure and mechanical behavior of T91 weld metal before and after an irradiation in SINQ Target-3. Optical and TEM observations and micro-hardness tests were performed to identify the irradiation effects. Before irradiation, the micro-structure of the T91 weld metals consisted of mainly tempered martensite and retained ferrite area. Precipitates in the weld metal are predominately M_7C_3 carbides, and few $M_{23}C_6$ particles are observed along the martensitic lath and primary austenite grain boundaries. The dislocation density in the weld metal is much higher than that in the base metal. The main feature of the irradiated micro-structure of the weld metal are small defects (black dots) and faulted Frank interstitial loops at lower irradiation temperature and a high density of helium bubbles appear at higher irradiation dose and temperature. The results are comparable with those of the T91 base metal irradiated under the same condition in the previous work. The weld metal and heat affected zone (HAZ) show much higher hardness than the base metal before irradiation, showing that no post-weld heat treatment (PWHT) has been applied to the weld metal. Irradiation hardening increases with irradiation dose below 10 dpa, but decreases at higher dose, which might be related to the transformation of M_7C_3 precipitates to $M_{23}C_6$ at higher irradiation temperatures.

1. Introduction

Due to its high strength at elevated temperatures, lower thermal stress and anticipated low liquid metal corrosion rates, the conventional martensitic steel T91 is now one candidate structural material for the container of liquid targets of spallation neutron source [1,2].

Welding is required for the fabrication of components. Post-irradiation properties of welds are therefore of much interest for designers. A lot of work has been done on the micro-structure and mechanical properties of weld metal of ferrite-martensitic stainless steels like F82H and T91, but most were concerned mainly with the mechanical properties before and after neutron irradiation [3–8]. This study evaluates the micro-structure and properties of T91 weld metal after an irradiation in the Swiss spallation neutron source (SINQ) Target-3 under a proton and neutron mixed spectrum. The results are compared with a previous results of F82H weld metal under the same irradiation condition.

2. Experiment

T91 steel (Heat 30176) received from Oak Ridge national laboratory has a composition of 8.32 Cr, 0.86 Mo,

* Corresponding author. Tel.: +41 56 3104491; fax: +41 56 3104529.
E-mail address: xuejun.jia@psi.ch (X. Jia).

0022-3115/$ - see front matter © 2005 Elsevier B.V. All rights reserved.
doi:10.1016/j.jnucmat.2004.10.171

Table 1
Irradiation condition and defect TEM measurement results for T91 weld

Specimen	Dose (dpa)	Helium (appm)	H (appm) (calculated)	Irradiation temperature (°C)	Defect size (nm)	Defect density (m^{-3})	Bubble size (nm)	Bubble density (m^{-3})
K^{16}	3.8	214	1490	110 ± 10	3.9	3.48×10^{22}	–	–
K^{7}	5.8	368	1928	210 ± 10	3.9	3.91×10^{22}	–	–
K^{11}	9.1	668	3330	245 ± 20	4.4	4.22×10^{22}	1.0	5.53×10^{23}
K^{21}	10.4	738	3730	295 ± 20	5.2	5.33×10^{22}	1.1	5.33×10^{23}
K^{19}	11.5	1075	4860	360 ± 30	8.1	1.60×10^{22}	1.4	5.28×10^{23}

0.48 Mn, 0.20 V, 0.06 Ni, 0.06 Nb and 0.09 °C, in wt%, and Fe for the balance. The plate was cold-rolled from 6 mm to 3 mm in thickness, and was subjected to a heat treatment: normalized at 1040 °C for 1 h, rapidly cooled and tempered at 750 °C for 1 h [9]. The 3 mm-thick plate was EB-welded without filler metal. The welding speed was about 760 mm/min with an electron beam of 125 kV and 6.5–7.0 mA.

TEM disc samples containing the weld area were used in the present study to perform both micro-structure observation and micro-hardness tests. The discs were irradiated to 2–12 dpa. The irradiation temperature varied from 110 °C to 360 °C due to the different positions of the samples in the target. One thing should be noted is that the irradiation temperature is increased with increasing irradiation dose. More detailed information can be found in Ref. [10]. Table 1 summarizes the information of irradiation doses and temperatures of the samples.

Samples for optical examination were prepared by polishing and etching in Villela reagent. Micro-hardness test was performed by means of Vickers micro-hardness measurements ($HV_{0.05}$) on 3 mm TEM discs. Transmission electron microscope (TEM) samples preparation was optimized by using 1 mm techniques, in which the 1 mm disk is punched from the center of the welded zone after etching. TEM investigation of the micro-structure was performed at 200 kV on a JEOL 2010 equipped with EDX measurement device. The most often used image conditions were bright field (BF) and weak beam dark-field (WBDF) at g ($4g$–$6g$), $g = 200$ near $z = 011$. But only micro-graphs of g ($5g$) were used for quantifying the size and density of defect clusters [11].

3. Results and discussion

3.1. Metallurgical characterizations

Fig. 1(a) shows the cross-sections of the EB welded T91 plate taken from a TEM sample. The width of the weld zone and HAZ is 1 mm and 0.3 mm, respectively. The mean grain size of the base metal is about 30 μm. In the welded zone, the coarse grains are more irregular and the mean grain size is above 50 μm. Fig. 1(b) and (c) show the grain structures of the base and welded zone metals; both of them are fully martensitic structure with several martensite laths bundles with different orientations in any one grain.

3.2. Micro-hardness test

Micro-hardness was measured perpendicularly to the weld center along a line from base metal (BM), HAZ and welded zone, see Fig. 1(a). The hardness value of T91 base metal is around 220 HV measured with a weight of 0.05 N, the holding time of loading in the testing is 20 s. Hardening in the weld metal and the adjacent HAZ is more clearly observed and gives a value about 460–490 HV, and the hardness in the HAZ region is the highest (see Fig. 2).

Normally, for martensitic steels, the post-weld heat treatment (PWHT) should be performed immediately after the welding. This will reduce the welding stresses, improve the toughness and stabilize the micro-structure of the weld metal. After the PWHT, the micro-hardness of the weld metal will be recovered and gives a value about 300 HV [8]. Such a high hardness value (460–490 HV) in the weld and HAZ area suggests that the PWHT was not performed on the T91 weld samples used in this work.

After irradiation, significant irradiation hardening was found by the micro-hardness test. The hardness of the weld metal increases with increasing dose up to about 10 dpa, then start to decrease, as shown in Fig. 3. The previous result of the F82H weld is also plotted in Fig. 3 for a comparison. It shows that the T91 weld has a different dose dependence of irradiation hardening compared to F82H weld metal, which does not show saturation up to 11.4 dpa similar to the tensile test results obtained from several ferritic/martensitic steels irradiated with high-energy protons [12–14].

3.3. Micro-structure

The micro-structure of the T91 weld metal consisted of mainly tempered martensite and retained ferrite area. Precipitates in the weld metals are predominately high-

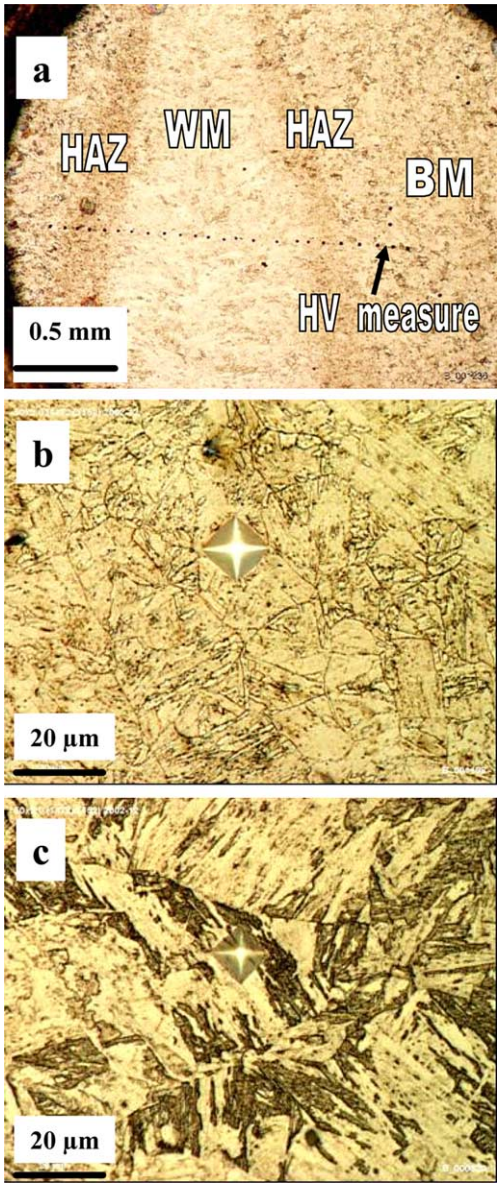

Fig. 1. (a) The cross-section of the EB welded T91 plate, the optical micro-structure of the base metal (b) and the weld metal (c).

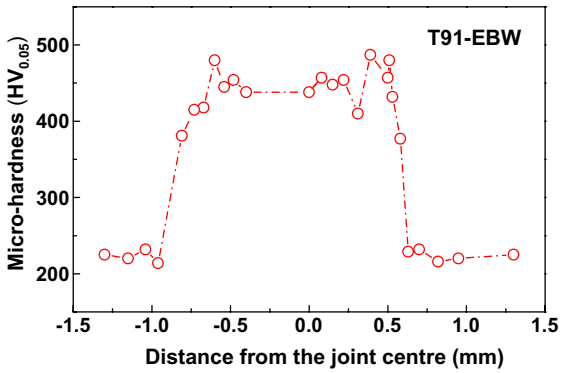

Fig. 2. Micro-hardness measurement of T91 steel along the line from the base metal to the weld metal before irradiation (see Fig. 1).

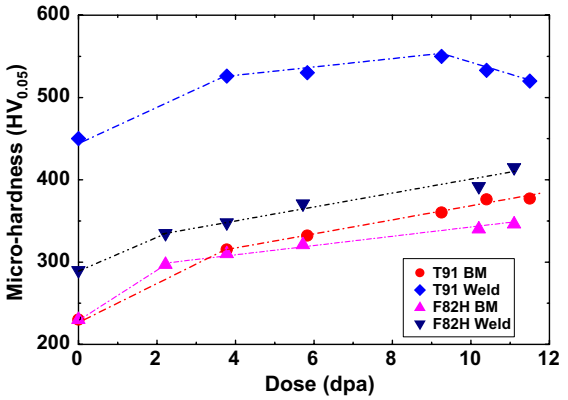

Fig. 3. Micro-hardness of the T91 and F82H base and weld metal as a function of irradiation dose. The data of F82H are from a previous work [16,17].

density plate-like carbides with sizes of about 100–200 nm in the retained ferrite area and few $M_{23}C_6$ particles are observed along the martensitic lath boundaries and primary austenite grain boundaries. Fig. 4(a)–(d) show the martensitic lath micro-structure of the T91 base metal and the weld metal before irradiation. The main difference between the weld metal and the base metal is that there are very few $M_{23}C_6$ precipitates along the lath and grain boundaries in the weld metal and the dislocation density in the weld metal of about 2.8×10^{14} m^{-2}, is much higher than in the base metal ($\approx 1.2 \times 10^{14}$ m^{-2}).

Fig. 5(a) shows the retained ferrite area in the weld metal. During the cooling of the weld metal, due to the enrichment of Cr, Mo and other ferrite stabilizing elements in the δ-ferrite, some δ-ferrite would remain to room temperature. High-density plate-like precipitates are found inside the retained ferrite area and also within the martensitic lath (Fig. 5(b)). As the precipitates plates are very thin, the EDX analysis could not be carried out to figure out their composition by TEM.

In most steels, M_7C_3 and $M_{23}C_6$ (M = Cr and Fe) are the most common precipitates in steels contains certain Cr and low carbon. X-ray diffractometry (XRD) analysis on particles extracted from the meld zone of welds of ferrite-martensitic steels like F82H, JLF-1 or Optifer steels evidenced the presence of different types of carbides, in particular of the Cr-rich carbides M_7C_3 and $M_{23}C_6$ [8]. The relative amount of Cr-rich carbides de-

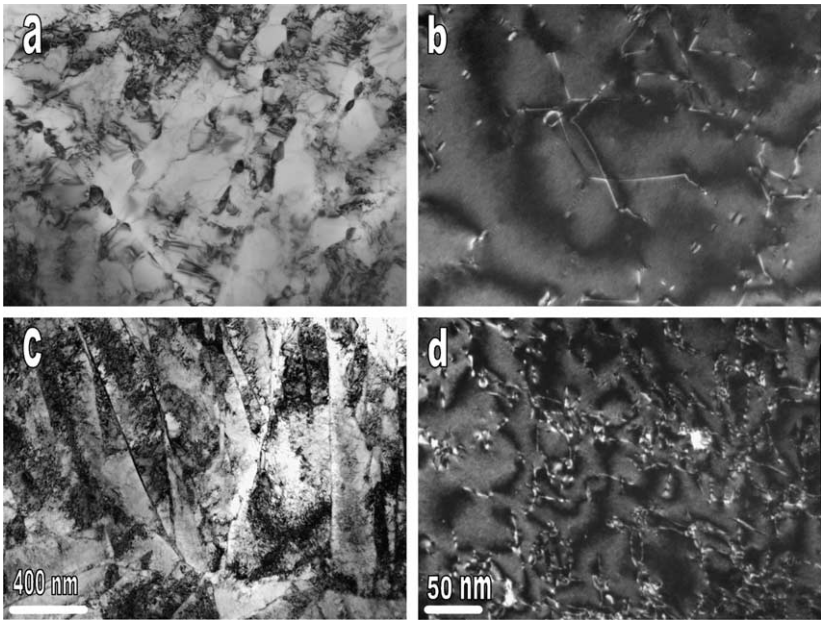

Fig. 4. The micro-structure of the T91 base and weld metals before irradiation. (a) Base metal, BF image, (b) base metal, WBDF image, (c) weld metal, BF image and (d) weld metal, WBDF image.

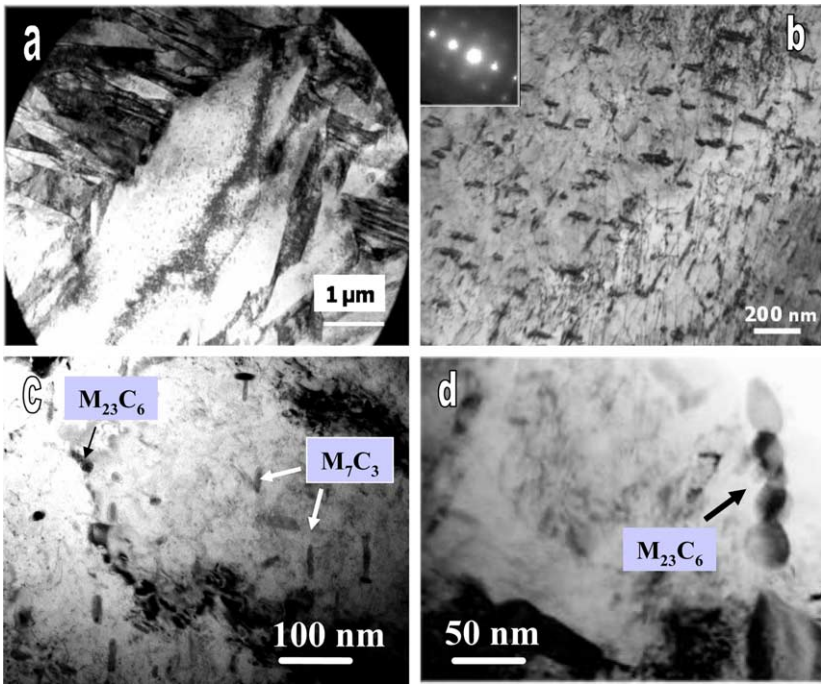

Fig. 5. The retained ferrite area in the weld metal (a), the precipitate structure in the retained ferrite area (b) and the precipitates structure after irradiation at 360 °C (c,d).

pends on the cooling rate of the weld metal; due to the faster cooling rate of EBW technique, the temperature range at which $M_{23}C_6$ precipitates form (600–750 °C) is crossed too quickly, so that nearly no $M_{23}C_6$ is found in the present T91-EBW weld metal, and precipitates are predominately M_7C_3 carbides.

The present results show the decrease of hardness occurs at irradiation temperature above about 300 °C (see Fig. 3). Meanwhile, TEM results show that the lower density of M_7C_3 carbides. At the same time, coarse $M_{23}C_6$ precipitates which were identified by the diffraction patterns under TEM with a fcc crystal structure of a lattice parameter of 1.07 nm, are observed along the martensitic lath boundaries, see Fig. 5(c) and (d). Normally, the M_7C_3 precipitates in the weld metal are stable at tempering temperature lower than 500 °C. At the tempering temperature above 600 °C, the M_7C_3 will coarsen and will be replaced by $M_{23}C_6$ precipitates, which nucleate on the martensitic lath and primary austenite grain boundaries, leading to a decrease of hardness and also the decrease of dislocation density. The present results show that the transformation of carbides structures and a decrease of hardness occur at irradiation temperature above about 300 °C. The reason is not cleared yet, probably due to the irradiation assisted the transformation of M_7C_3 to $M_{23}C_6$ at higher irradiation temperatures.

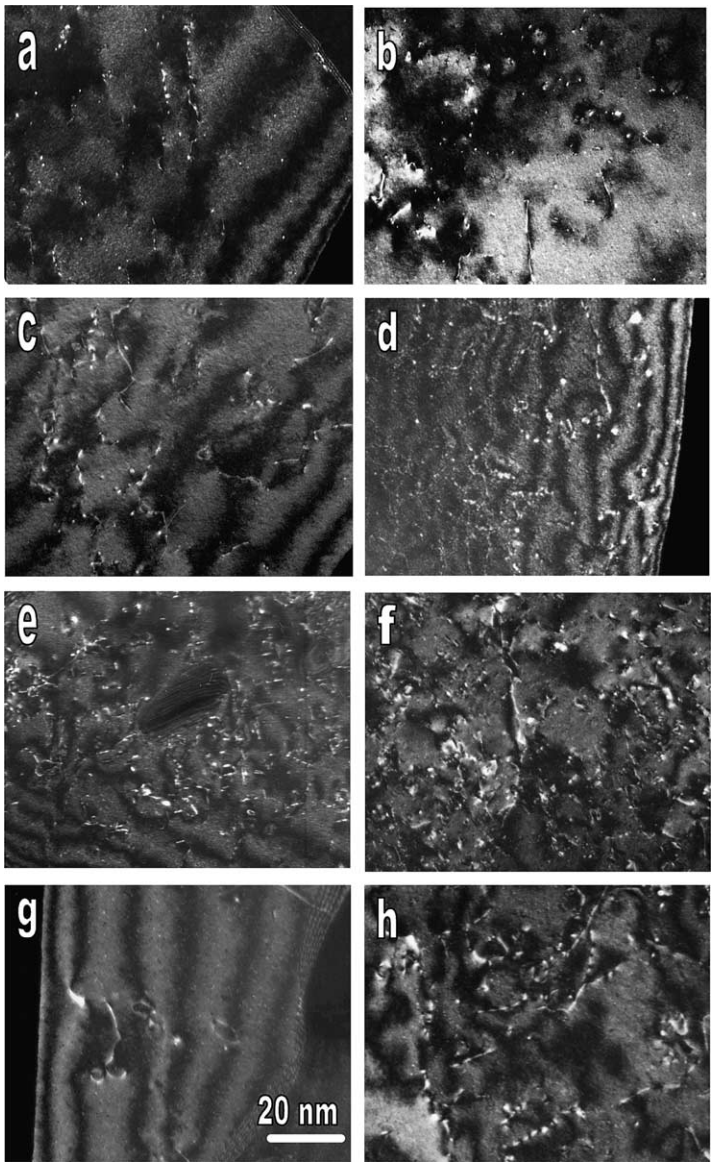

Fig. 6. The micro-structure of the T91 base and weld metal after irradiation. For base metal: (a) 3.8 dpa/110 °C, (c) 5.8 dpa/220 °C, (e) 10.1 dpa/255 °C and (g) 11.8 dpa/360 °C, and for weld metal: (b) 3.8 dpa/110 °C, (d) 5.8 dpa/210 °C, (f) 10.4 dpa/275 °C and (h) 11.5 dpa/350 °C, respectively.

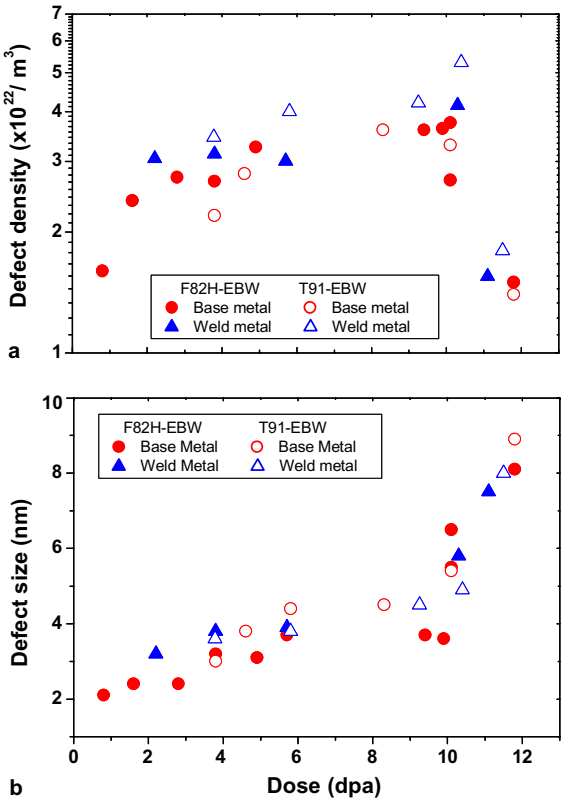

Fig. 7. Dose dependence of the size (a) and density (b) of defect clusters in T91 weld metal. The data of F82H base and weld metal and of T91 base metal from the previous work [11,16,17] are plotted for comparison.

Fig. 6(a)–(h) shows the irradiated micro-structures of T91-EBW, together with our previous results for the T91 base metal irradiated under the same conditions [14]. The comparison shows that there is not much difference between the radiation-induced defect cluster structures. Namely, at low irradiation dose and temperature, micro-structure is dominated by very small defect clusters (black dots or small interstitial loops [15]), as shown in Fig. 6(a) and (b). With increasing irradiation dose, the defect cluster size and density increase, as show in Fig. 6(c)–(f). But at the highest irradiation does, see Fig. 6(g) and (h), because of the higher irradiation temperature, the defect density decreases and the mean size increases significantly.

Fig. 7 gives the dose dependence of the size and density of defect clusters in the T91-EBW weld metal. The data of the F82H and T91 base metal and the F82H weld metal from previous results [16,17] was also plotted for a comparison. Both materials give similar results and also the densities and the mean sizes of defect clusters in the weld metal are comparable with those in the base metal.

As observed in the base metal, helium bubble structure was also found in the weld metal at higher irradiation doses with higher irradiation temperature, as shown in Fig. 8. Compared to the base metal which has a bubble density of about $\sim 5 \times 10^{23}$ m^{-3} [16], the bubble density was slightly higher in the weld metal as a result of the higher dislocation density. These dislocations act as sinks for the irradiation produced interstitials and interstitial clusters and allow the vacancies to aggregate to form small voids; these small voids finally become the sinks for the transmutation helium produced under spallation conditions. On the other hand, the mean bubble size is similar to that of the base metal. This result is also comparable with the previous results for F82H steels [11,16,17].

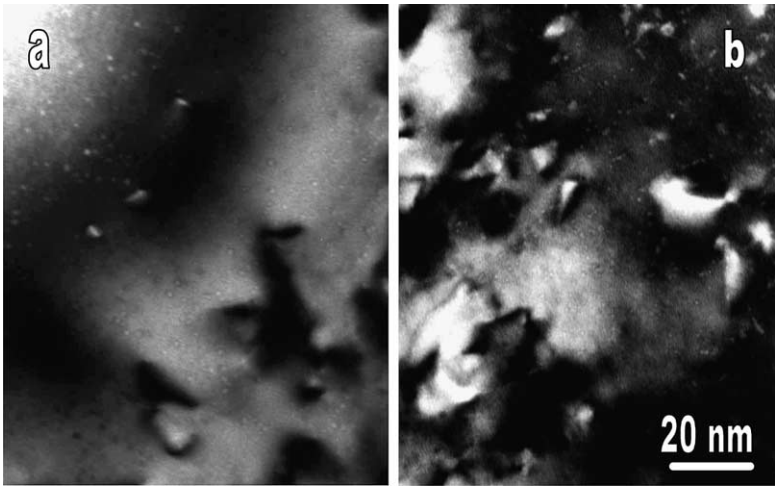

Fig. 8. Helium bubble structure in T91 steel after irradiation: (a) base metal, 10.1 dpa/255 °C and (b) weld metal, 10.4 dpa/275 °C.

4. Conclusions

1. Before irradiation, the micro-structure of the T91 weld metal consisted of mainly tempered martensite and retained ferrite area. Precipitates in the weld metal are predominately M_7C_3 carbides, and few $M_{23}C_6$ particles are observed along the martensitic lath boundaries and primary austenite grain boundaries. The dislocation density in the weld metal is much higher than in the base metal.
2. The main feature of the irradiated micro-structure in the weld metal are small defects (black dots) and faulted Frank loops at lower irradiation temperatures, while a high density of helium bubbles appears additionally at higher irradiation doses and temperatures. The results are comparable to those of the T91 base metal and also to the F82H steel irradiated under the same conditions in a previous work.
3. Micro-hardness test results shows much higher hardness in the weld metal and heat affected zone (HAZ) than in the base metal before irradiation, showing that the post-weld heat treatment (PWHT) was not applied to the weld metal. The irradiation hardening increases with irradiation dose, but decreases at irradiation temperature above about 300 °C, which might be related to the transformation of M_7C_3 precipitates to $M_{23}C_6$ at higher irradiation temperature.

Acknowledgment

This work is included in SPIRE (Irradiation effects in martensitic steels under neutron and proton mixed spectrum) program, a subprogram of the European 5th Framework Program, which is supported by Swiss Bundesamt fuer Bildung und Wissenschaft.

References

[1] G.S. Bauer, M. Salvatores, G. Heusener, J. Nucl. Mater. 296 (2001) 17.
[2] Y. Dai, ICANS-XII and 4th Plenary Meeting of the ESS Project (ESS-PM4), 1995.
[3] R. Mythili, V. Thomas Paul, S. Saroja, M. Vijayalakshmi, V.S. Raghunathan, J. Nucl. Mater. 312 (2003) 199.
[4] A. Alamo, A. Castaing, A. Fontes, P. Wident, J. Nucl. Mater. 283–287 (2000) 1192.
[5] T. Sawai, K. Shiba, A. Hishinuma, J. Nucl. Mater. 283–287 (2000) 657.
[6] G.J. Cai, Microstructure and mechanical properties of high chromium steel weld metals, Thesis no. 1012, Goeteborg, Sweden, 1994.
[7] J. Rensman, E.V. van Osch, M.G. Horsten, D.G. d'Hulst, J. Nucl. Mater. 283–287 (2000) 1201.
[8] G. Filacchioni, R. Montanari, M.E. Tata, L. Pilloni, J. Nucl. Mater. 307–311 (2002) 1563.
[9] K. Farrell, private communication.
[10] Y. Dai, G. Bauer, J. Nucl. Mater. 296 (2001) 43.
[11] X. Jia, Y. Dai, M. Victoria, J. Nucl. Mater. 305 (2002) 1.
[12] R. Klueh, D.R. Harries, High-chromium ferritic and martensitic steels for nuclear Application, ASTM stock number: MONO3, ISBN 0-8031-2090-7.
[13] Y. Dai, X. Jia, K. Farrell, J. Nucl. Mater. 318 (2003) 192.
[14] K. Farrell, T.S. Byun, J. Nucl. Mater. 318 (2003) 274.
[15] D.S. Gelles, J. Nucl. Mater. 233–237 (1996) 293.
[16] X. Jia, Y. Dai, J. Nucl. Mater. 318 (2003) 207.
[17] X. Jia, Y. Dai, J. Nucl. Mater. 329–333 (2004) 309.